 doi:10.20944/preprints202207.0074.v1

Properties of bound electron pairs

Jacob Szeftel
ENS Paris-Saclay/LuMIn, 4 avenue des Sciences, 91190 Gif-sur-Yvette, France

The energies of spin singlet and triplet *bound* electron pairs are reckoned for electrons interacting through the Coulomb interaction, while sitting on neigbouring lattice sites. It is concluded that *triplet* pairs are unlikely to be observed due to screening. The interplay of inter-electron couplings of *different* spatial range is investigated. High-pressure induced superconductivity is analysed and *qualitative agreement* is achieved with observed results by working out the dependence of the critical temperature on the microscopic parameters, characterising the electron motion. This approach can be applied to other kinds of inter-electron interactions.

PACS numbers: 74.20.Fg,74.20.Rp

I. INTRODUCTION

The paramount role of bound electron pairs in superconductivity[1,2] has ever been known since Cooper's seminal work[3], even though assuming an *attractive* interaction between electrons, as done by Cooper and furthermore by BCS[4], has been shown to be *inconsistent* with persistent currents[5], thermal equilibrium[6], occurrence of a second order transition[7,8] at the critical temperature T_c and the Josephson effect[9]. Nevertheless it has been established[6] that the bound electron pair of energy ε_B turns *continuously* into a many bound electron (*MBE*) state, carrying persistent currents, at *finite* electron concentration c_s. In particular, there is[5,6]

$$\mu(c_s = 0) = \frac{\varepsilon_B}{2} \quad ,$$

with $\mu(c_s)$ being the chemical potential of superconducting electrons, making up the *MBE* state. Besides describing the inter-electron coupling by means of the Hubbard Hamiltonian[3,4,6,8] entails, as a consequence of Pauli's principle, that the spin of any bound pair can be but equal to 0 and the ensuing *MBE* state has thence vanishing spin too, which has been confirmed experimentally[1,2]. However this broaches the issue of why it is so, because, as shown below, triplet pairs do indeed arise, if electrons, sitting on neighbouring sites, are allowed to interact.

Yet, opposing the hereabove statement, experimental evidence of spin triplet pairs was reported[10,11] in superconducting materials of type II, subjected to a magnetic field H, giving rise to a vortex lattice. Actually, it was inferred from the magnetisation M being temperature independent, while crossing T_c. However, due to the Meissner effect, H and thence M are bound to *vanish* in bulk superconducting matter. Furthermore, the *macroscopic* susceptibility should be *diamagnetic*, as resulting from Lenz's law[12–14], and weak with respect to the *paramagnetic* (Pauli-like) one, associated with the spin of normal electrons[15], and it ought to have thence the *opposite* sign. Therefore, the most likely conclusion is that the measurements[10,11] have actually probed but the magnetisation of *normal* electrons inside the *vortices*.

Another topic of significance is pressure proving instrumental on T_c, particularly after the recent discovery of high-pressure induced superconductivity at room-temperature[16–18]. It has been known[19] for long that pressure gives rise to opposite trends in low- and high-T_c superconductors, respectively. Regarding these materials, exhibiting no isotope effect, no cogent explanation has been offered so far, whereas a theory, based on Eliashberg's work[20], has been widely used for those which do so. Unfortunately it relies heavily on the BCS theory[4], which has been proved to be marred[5–9] by major inconsistencies, recalled above. Likewise a *cornerstone* assumption of the BCS scheme[4] requires that the electron-phonon interaction reverse the *sign* of the Coulomb repulsive force and thus give rise eventually to an effective, *attractive* coupling between two electrons, located on the *same* atomic site. However a more accurate treatment[7] has disproved such a statement. Therefore this work is also intended at investigating how pressure alters the microscopic parameters[8], governing the motion of electrons coupled through the Coulomb interaction, and assigns thereby T_c.

The outline is as follows: section II deals with the properties of bound pairs, resulting from first neighbour electrons, coupled through the Coulomb repulsion; the role of the interaction range is elucidated in section III, while high-pressure induced superconductivity is addressed in section IV; the physical significance of this work is stressed in the conclusion.

II. BOUND ELECTRON PAIRS

For simplicity, a one-dimensional ($d = 1$) lattice, containing $N >> 1$ of atomic sites labelled by index $i = 1, ..N$, is considered. The lattice parameter is taken equal to unity and each site can accommodate at most two electrons of opposite spin $\sigma = \pm 1/2$. The Hamiltonian H_1 then reads

$$\begin{array}{l} H_1 = \sum_{i,j,\sigma} \left(\frac{t}{2} \left(c^+_{i,\sigma} c_{j,\sigma} + c^+_{j,\sigma} c_{i,\sigma} \right) \right. \\ + \left(U_1 - J \right) c^+_{i,\sigma} c^+_{j,\sigma} c_{j,\sigma} c_{i,\sigma} \\ \left. + U_1 c^+_{i,\sigma} c^+_{j,-\sigma} c_{j,-\sigma} c_{i,\sigma} - J c^+_{i,\sigma} c^+_{j,-\sigma} c_{j,\sigma} c_{i,-\sigma} \right) \end{array} ,$$

wherein the sum is carried out over $\sigma = \pm$, $i = 1, ..N-1$ with $j = i+1$ and $c^+_{i,\sigma}, c_{i,\sigma}$ are one-electron creation and

Preprints (www.preprints.org) | NOT PEER-REVIEWED | Posted: 5 July 2022 doi:10.20944/preprints202207.0074.v1

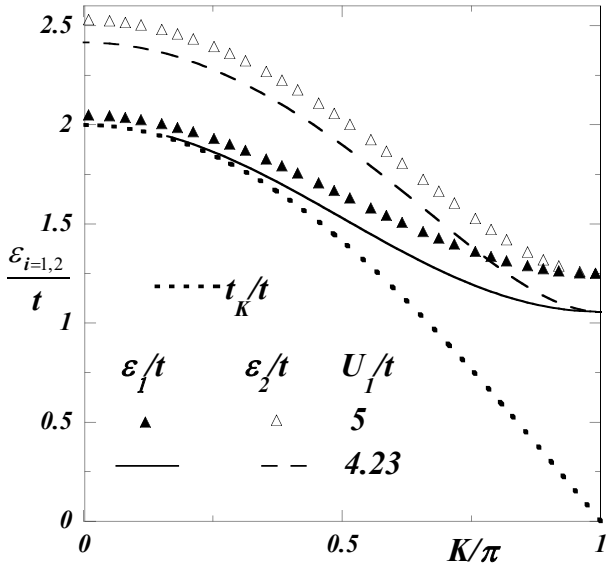

FIG. 1. Plots of $t_K = 2t\cos\left(\frac{K}{2}\right)$ (dotted line) and eigenvalues of H_1, $\varepsilon_1(K)$ (solid line and black triangle) and $\varepsilon_2(K)$ (dashed line and white triangle), reckoned for $K \in [0,\pi]$ and various U_1 values with $J = U_1/10$ for triplet pairs.

annihilation operators on the Wannier[15] state $|i,\sigma\rangle$

$$|i,\sigma\rangle = c^+_{i,\sigma}|0\rangle \quad , \quad |0\rangle = c_{i,\sigma}|i,\sigma\rangle \quad ,$$

with $|0\rangle$ being the no electron state. Then $\frac{t}{2}, U_1, J$ designate the hopping, Coulomb and exchange integrals, respectively

$$\begin{array}{l} t = 2\langle 0|\, c_{j,\sigma} V_{e-n} c^+_{i,\sigma}|0\rangle \\ U_1 = \langle 0|\, c_{j,-} c_{i,+} V_{e-e} c^+_{i,+} c^+_{j,-}|0\rangle \\ J = \langle 0|\, c_{j,+} c_{i,-} V_{e-e} c^+_{i,+} c^+_{j,-}|0\rangle \end{array} \quad ,$$

with V_{e-n}, V_{e-e} referring to the electron-nucleus and electron-electron Coulomb potentials, respectively. Note that there is in general $|J| << U_1$, due to the Wannier wave-functions decaying exponentially[15] with growing inter-atomic distance.

It is convenient to recast H_1 into momentum space. To that end, let us first recall the definitions of the one-electron creation and annihilation operators on the Bloch[15] state $|k,\sigma\rangle$

$$|k,\sigma\rangle = c^+_{k,\sigma}|0\rangle \quad , \quad |0\rangle = c_{k,\sigma}|k,\sigma\rangle \quad ,$$

with k being any vector of the Brillouin zone, fulfilling periodic boundary conditions. They enable us to introduce the pair creation and annihilation operators[6,21]

$$\begin{array}{ll} b^+_{s,K,k} = c^+_{k,+} c^+_{K-k,-} & , \quad b_{s,K,k} = c_{K-k,-} c_{k,+} \\ b^+_{t,K,k} = c^+_{k,\sigma} c^+_{K-k,\sigma} & , \quad b_{t,K,k} = c_{K-k,\sigma} c_{k,\sigma} \end{array} \quad ,$$

with K being any vector of the Brillouin zone and the subscripts s,t referring to *singlet* and *triplet*, because the spin ζ of the corresponding electron pair, projected onto any axis, is equal to $0, \pm 1$, respectively. The hereabove definitions deserve some further comments :

- those pair operators are neither bosons, nor fermions, but the operational rules, governing their algebraic properties, will be given below in section IV;

- the notation s,t, albeit convenient, is not exact, because the true singlet and triplet pair states with $\zeta = 0$, read actually $\left(b^+_{s,K,k} \pm b^+_{s,K,K-k}\right)|0\rangle$.

Then H_1 reads in momentum space

$$\begin{array}{l} H_1 = H_d + \sum_K \left(H^t_K + H^s_K\right) \\ H_d = \sum_{k,\sigma} \epsilon(k) c^+_{k,\sigma} c_{k,\sigma} \quad , \quad \epsilon(k) = t\cos(k) \\ H^t_K = \sum_{k,k'} \frac{V^t_{K,k,k'}}{N} b^+_{t,K,k} b_{t,K,k'} \\ V^t_{K,k,k'} = (U_1 - J)\cos(k-k') \\ H^s_K = \sum_{k,k'} \frac{V^s_{K,k,k'}}{N} b^+_{s,K,k} b_{s,K,k'} \\ V^s_{K,k,k'} = 2\left(U_1\cos(k-k') + J\cos(K-k-k')\right) \end{array} \quad , \quad (1)$$

where the sums over K, k, k' are to be carried out over the whole Brillouin zone. The Hamiltonian H_d describes the motion of independent electrons of one-electron energy $\epsilon(k)$, whereas H^t_K, H^s_K account for two-electron scattering of triplet and singlet pairs, respectively. Due to Pauli's principle, there is $V^t_{K,k,k'} \neq V^s_{K,k,k'}$, so that the outcome of two-electron scattering *differs*[21] according to whether the incoming electrons have *same* or *opposite* spin direction, although the Coulomb interaction is *spin-independent*.

Because of $H^{\alpha'}_K b^+_{\alpha,K,k}|0\rangle = 0$ if $K \neq K'$ or $\alpha \neq \alpha'$, each solution ψ, ε of the Schrödinger equation, written for a *single* pair,

$$\left(H_d + H^{\alpha=t,s}_K - \varepsilon\right)\psi = 0$$

is also a solution[21] of

$$\left(H_1 - \varepsilon\right)\psi = 0 \quad .$$

Besides, triplet pairs are such that $b^+_{t,K,k} = -b^+_{t,K,K-k}$, which entails $\sum_k = \frac{N}{2}$, by contrast with singlet pairs for which there is $b^+_{s,K,k} \neq b^+_{s,K,K-k} \Rightarrow \sum_k = N$. Two consequences can be deduced from this property

- the Schrödinger equation for one singlet pair has twice more solutions than for one triplet pair;

- the following identity ensues for any function $f(k)$ in case of $N \to \infty$

$$\sum_k \frac{f(k)}{N} = \int_{-\pi}^{\pi} f(k)\rho(k)dk \quad ,$$

with $\rho(k) = \frac{1}{4\pi}$ and $\rho(k) = \frac{1}{2\pi}$ for triplet and singlet pairs, respectively.

Let us begin with solving the Schrödinger equation for

Preprints (www.preprints.org) | NOT PEER-REVIEWED | Posted: 5 July 2022 doi:10.20944/preprints202207.0074.v1

one triplet pair

$$\begin{array}{l}(H_d+H_K^t-\varepsilon(K))\,\psi=0, \psi=\sum_k a(k)b^+_{t,K,k}\,|0\rangle \\ a(k)=\sum_{k'} a(k')\frac{V^t_{K,k,k'}}{N(\varepsilon(K)-\varepsilon(K,k))} \\ \varepsilon(K,k)=\epsilon(k)+\epsilon(K-k)\end{array}\Bigg\}\Rightarrow$$
$$\begin{cases}\frac{a(k)}{U_1-J}=\frac{\cos(k)\Delta_c+\sin(k)\Delta_s}{\varepsilon(K)-\varepsilon(K,k)} \\ \Delta_c=\sum_k \frac{a(k)\cos(k)}{N}, \quad \Delta_s=\sum_k \frac{a(k)\sin(k)}{N}\end{cases} \quad . \quad (2)$$

Eq.(2) can then be recast as a homogeneous system of two linear equations in terms of two unknowns Δ_c, Δ_s

$$\begin{array}{l}\Delta_c\left(\frac{1}{U_1-J}-S_{cc}\right)-\Delta_s S_{cs}=0 \\ \Delta_c S_{cs}+\Delta_s\left(S_{ss}-\frac{1}{U_1-J}\right)=0\end{array} \quad , \quad (3)$$

with S_{cc}, S_{cs}, S_{ss} defined as follows in case of $N\to\infty$

$$\begin{array}{c}S_{cc}=\int_{-\pi}^{\pi}\frac{\cos^2(k)}{\varepsilon(K)-\varepsilon(K,k)}\frac{dk}{4\pi}, \quad S_{ss}=\int_{-\pi}^{\pi}\frac{\sin^2(k)}{\varepsilon(K)-\varepsilon(K,k)}\frac{dk}{4\pi} \\ S_{cs}=\int_{-\pi}^{\pi}\frac{\sin(2k)}{\varepsilon(K)-\varepsilon(K,k)}\frac{dk}{8\pi}\end{array} \quad .$$

Finally, $\varepsilon(K)$ is found by equating to 0 the determinant of the system in Eq.(3). Let $\pm t_K$ be the maximum and minimum of $\varepsilon(K,k)$ over k. Then Eq.(3) has, for $U_1>0$, at most two solutions $t_K<\varepsilon_1(K)<\varepsilon_2(K)$, associated with a *bound* pair and $\frac{N}{2}-2$ of solutions, making up the continuum $[-t_K, t_K]$ and corresponding to two-electron *scattering* states. The dispersion curves $\varepsilon_1(K), \varepsilon_2(K)$ merge for $K=\pi$ into a single twofold degenerate value $=\frac{U_1-J}{4}$. The results $\varepsilon_1(K), \varepsilon_2(K)$ have been plotted in Fig.1. Remarkably, regarding the solid line, there is no ε_1 for $K_m<.15\pi$ and no solution $\varepsilon_{i=1,2}(K\in[0,\pi[)$ can be found at all for $\frac{U_1}{t}<4.1$. This is in marked contrast with the Hubbard Hamiltonian, for which there is a bound electron pair in one and two dimensions, even though the on-site Coulomb integral

$$U_0=\langle 0|\,c_{i,-}c_{i,+}V_{e-e}c^+_{i,+}c^+_{i,-}\,|0\rangle$$

goes[3,6,8] down to 0. Due to screening, there is $U_1<U_0/5$, so that $U_1>5t$ is unlikely to occur in metals because of $U_0\approx t$. Finally it is impossible to have $\frac{U_1}{t}>4.23$, which accounts for no triplet bound pair being indeed observed[1,2] in any superconductor.

The singlet pair eigenvalues will be calculated too, because they are needed for the next section. The Schrödinger equation reads then

$$\begin{array}{l}(H_d+H_K^s-\varepsilon(K))\,\psi=0, \psi=\sum_k a(k)b^+_{s,K,k}\,|0\rangle \\ a(k)=\sum_{k'} a(k')\frac{V^s_{K,k,k'}}{N(\varepsilon(K)-\varepsilon(K,k))}= \\ 2\frac{\Delta_c(U_1\cos(k)+J\cos(K-k))+\Delta_s(U_1\sin(k)+J\sin(K-k))}{\varepsilon(K)-\varepsilon(K,k)}\end{array} \quad (4)$$

with $\varepsilon(K,k), \Delta_c, \Delta_s$ defined as in Eq.(2). Likewise Eq.(4) is recast into a homogeneous system of two linear equations in terms of the same unknowns Δ_c, Δ_s

$$\begin{array}{l}\Delta_c\left(U_1S_{cc}+J\left(\cos(K)S_{cc}+\sin(K)S_{cs}\right)-\frac{1}{2}\right)+ \\ \Delta_s\left(U_1S_{cs}+J\left(\sin(K)S_{cc}-\cos(K)S_{cs}\right)\right)=0 \\ \Delta_c\left(U_1S_{cs}+J\left(\cos(K)S_{cs}+\sin(K)S_{ss}\right)\right)+ \\ \Delta_s\left(U_1S_{ss}+J\left(\sin(K)S_{cs}-\cos(K)S_{ss}\right)-\frac{1}{2}\right)=0\end{array} \quad (5)$$

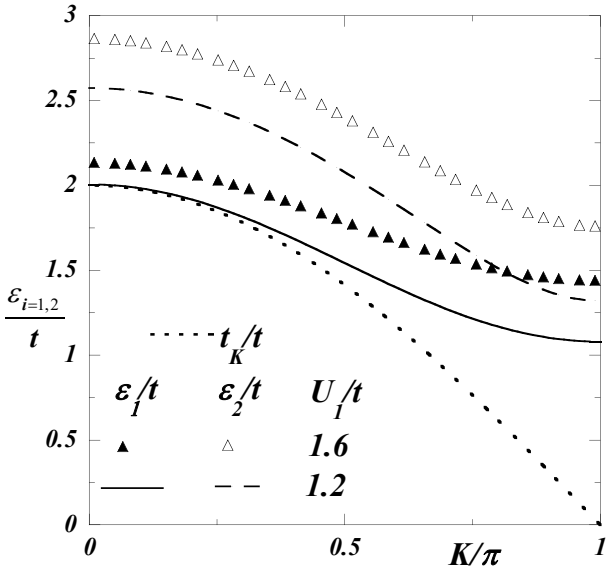

FIG. 2. Plots of t_K (dotted line) and eigenvalues of H_1, $\varepsilon_1(K)$ (solid line and black triangle) and $\varepsilon_2(K)$ (dashed line and white triangle), reckoned for $K\in[0,\pi]$ and various U_1 values with $J=U_1/10$ for singlet pairs.

with S_{cc}, S_{cs}, S_{ss} defined this time as follows for $N\to\infty$

$$\begin{array}{l}S_{cc}=\int_{-\pi}^{\pi}\frac{\cos^2(k)}{\varepsilon(K)-\varepsilon(K,k)}\frac{dk}{2\pi} \\ S_{cs}=\int_{-\pi}^{\pi}\frac{\sin(2k)}{\varepsilon(K)-\varepsilon(K,k)}\frac{dk}{4\pi} \\ S_{ss}=\int_{-\pi}^{\pi}\frac{\sin^2(k)}{\varepsilon(K)-\varepsilon(K,k)}\frac{dk}{2\pi}\end{array} \quad . \quad (6)$$

The resulting eigenvalues have been plotted in Fig.2. Similarly to Eq.(3), Eq.(5) has at most two solutions $\varepsilon_1(K)<\varepsilon_2(K)$, associated with a *bound* pair but, in contrast with triplet pairs, they are not degenerate at $K=\pi$, that is $\varepsilon_1(\pi)=U_1-J\neq\varepsilon_2(\pi)=U_1+J$. Likewise $\varepsilon_1(K), \varepsilon_2(K)$ vanish quickly for U_1/t decreasing under 1.2. Even though this threshold value, for a singlet pair to arise, is less demanding than for a triplet pair, a singlet pair, made up of electrons interacting on first neighbouring sites, is unlikely to be observed because of screening, too. However, it is of interest to study to which extent such a *weak* inter-electron coupling, embodied by $U_1<U_0, J<<U_0$, might modify the energy of a bound pair, stemming from the much *stronger* Hubbard interaction. This is the purview of the next section.

III. ROLE OF THE INTERACTION RANGE

Let us consider the Hamiltonian H_2, defined as

$$H_2=H_0+H_1-H_d \quad ,$$

where H_1, H_d are defined in Eqs.(1) and H_0 refers to the one-dimensional Hubbard Hamiltonian, recalled below[6,21]

$$H_0=H_d+\sum_K H^s_K, \quad V^s_{K,k,k'}=U_0, \quad \forall K,k,k' \quad .$$

Preprints (www.preprints.org) | NOT PEER-REVIEWED | Posted: 5 July 2022 doi:10.20944/preprints202207.0074.v1

Thus H_2 reads as expressed in Eqs.(1), but with U_0 being added to every $V^s_{K,k,k'}$. Conversely, H^t_K remains unaltered, because of $V^t_{K,k,k'} = 0, \quad \forall K, k, k'$ for H_0.

The Hubbard Hamiltonian has long been known to sustain one singlet bound pair[3,6] of energy $\varepsilon_0(K)$, obtained by solving the following equation[6,8]

$$\frac{2\pi}{U_0} = \int_{-\pi}^{\pi} \frac{dk}{\varepsilon_0(K) - \varepsilon(K,k)} \quad . \tag{7}$$

The dispersion of $\varepsilon_0(K)$ has been calculated for $U_0 = t$ and plotted in Fig.3. There is $\varepsilon_0(\pi) = U_0$. Though H_0 sustains a bound pair even for $U_0 \to 0$ in one and two dimensions[3,6,8], the prerequisite $\frac{U_0}{t_K} > .5$ must still be fulfilled[6,8] for a bound pair to arise in three dimensions.

Combining H_0 and H_1 will cause $\varepsilon_0(K)$ to shift to the singlet bound pair energy $\eta(K)$ of H_2, to be reckoned as follows

$$\begin{array}{l} (H_2 - \eta(K))\,\psi = 0, \quad \psi = \sum_k a(k) b^+_{s,K,k}\,|0\rangle \\ a(k)\,(\eta(K) - \varepsilon(K,k)) = U_0\Delta_0 + 2\,(\Delta_c\,(U_1\cos(k) \\ +J\cos(K-k)) + \Delta_s\,(U_1\sin(k) + J\sin(K-k))) \end{array} \tag{8}$$

with $\varepsilon(K,k), \Delta_c, \Delta_s$ defined as in Eq.(2) and Δ_0 reading

$$\Delta_0 = \sum_k \frac{a(k)}{N} \quad .$$

Eq.(8) can be recast as a homogeneous system of linear equations in terms of three unknowns $\Delta_0, \Delta_c, \Delta_s$

$$A \begin{bmatrix} \Delta_0 \\ \Delta_c \\ \Delta_s \end{bmatrix} = 0 \quad .$$

The 3×3 matrix A reads then

$$\begin{array}{l} A_{1,1} = U_0 S_0 - 1, \quad A_{2,1} = U_0 S_c, \quad A_{3,1} = U_0 S_s \\ A_{1,2} = 2\,(U_1 S_c + J\,(\cos(K) S_c + \sin(K) S_s)) \\ A_{1,3} = 2\,(U_1 S_s + J\,(\sin(K) S_c - \cos(K) S_s)) \\ A_{2,2} = 2\,(U_1 S_{cc} + J\,(\cos(K) S_{cc} + \sin(K) S_{cs})) - 1\ , \\ A_{2,3} = 2\,(U_1 S_{cs} + J\,(\sin(K) S_{cc} - \cos(K) S_{cs})) \\ A_{3,2} = 2\,(U_1 S_{cs} + J\,(\cos(K) S_{cs} + \sin(K) S_{ss})) \\ A_{3,3} = 2\,(U_1 S_{ss} + J\,(\sin(K) S_{cs} - \cos(K) S_{ss})) - 1 \end{array}$$

with S_0, S_c, S_s reading for $N \to \infty$

$$\begin{array}{c} S_0 = \int_{-\pi}^{\pi} \frac{dk}{2\pi(\eta(K) - \varepsilon(K,k))} \\ S_c = \int_{-\pi}^{\pi} \frac{\cos(k)}{\eta(K) - \varepsilon(K,k)} \frac{dk}{2\pi}, \quad S_s = \int_{-\pi}^{\pi} \frac{\sin(k)}{\eta(K) - \varepsilon(K,k)} \frac{dk}{2\pi} \end{array} .$$

S_{cc}, S_{cs}, S_{ss} are defined as in Eq.(6), but with $\eta(K)$ showing up instead of $\varepsilon(K)$. Finally the dispersion curve $\eta(K)$ is obtained by equating the determinant of A to 0. We have chosen to plot rather $e_0(K) = \frac{\eta(K)}{\varepsilon_0(K)} - 1$ in Fig.3, because the small, upward shift of ε_0 toward η, observed for the highest U_1 value, illustrates how barely the long range Coulomb coupling affects the pair energy obtained for the Hubbard model. Hence any interaction beyond first neighbours can be neglected because of screening. Besides, note that the curves $\varepsilon_{i=1,2}(K)$ of H_2 have merged into the continuum $[-t_K, t_K]$ because the chosen U_1 values are below the threshold $\frac{U_1}{t_K} \approx 1.2$.

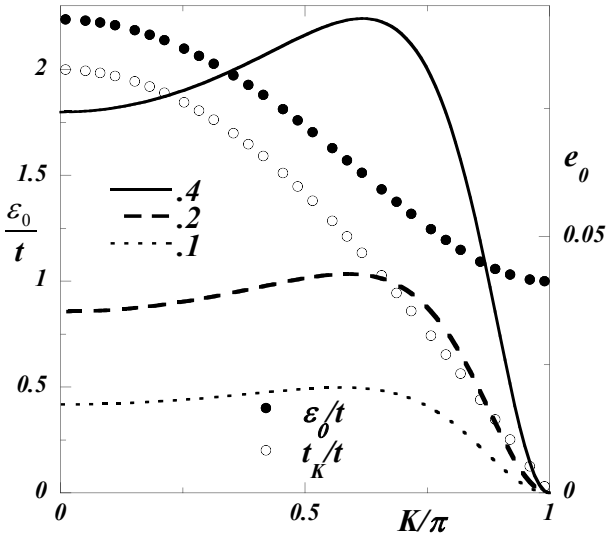

FIG. 3. Plots of t_K (white circle), $\varepsilon_0(K)$ (black circle) and $e_0(K) = \frac{\eta(K)}{\varepsilon_0(K)} - 1$, represented as a solid, dashed and dotted line, corresponding to $\frac{U_1}{U_0} = .4, .2, .1$ with $U_0 = t, J = U_1/10$, respectively; the scale for t_K, ε_0 is on the left hand side, but on the right hand side for e_0.

IV. ROLE OF PRESSURE

Pressure is expected to cause the lattice parameter to decrease and thence t to increase due to increasing overlap of Wannier wave-functions $c^+_{i,\sigma}\,|0\rangle\,, c^+_{i+1,\sigma}\,|0\rangle$, whereas U_0 is likely to be hardly altered, because it is almost independent from the lattice parameter. Thus let us begin with analysing the dependence of T_c upon decreasing U_0/t for the Hubbard Hamiltonian H_0. Hence, as done elsewhere[5–8], the conduction electrons are taken to comprise bound and independent electrons, in respective temperature dependent concentration $c_s(T), c_n(T)$, such that

$$c_0 = c_s(T) + c_n(T) \quad ,$$

with c_0 being the total concentration. The conduction electrons are organized as a many bound electron[6,8] (MBE) state and a Fermi gas[15], characterised, respectively, by the chemical potential $\mu(c_s)$ and the Fermi energy $E_F(T, c_n)$. Then the necessary conditions for a second order transition to occur at T_c read[7,8]

$$E_F(T_c, c_0) = \mu(0), \quad \rho'(E_F(T_c, c_0)) > 0 \quad , \tag{9}$$

$$\frac{\partial E_F}{\partial c_n}(T_c, c_0) = -\frac{\partial \mu}{\partial c_s}(0), \quad \frac{\partial E_F}{\partial c_n} > 0, \quad \frac{\partial \mu}{\partial c_s} < 0, \tag{10}$$

for which $\rho\,(\epsilon)\,, \epsilon$ refers to the one-electron density of states and energy[15] and $\rho'\,(\epsilon) = \frac{d\rho}{d\epsilon}$. Eq.(9) expresses the property that the set of conduction electrons is at *stable*, thermal equilibrium[5] at T_c, whereas Eq.(10) ensures that the *superconducting* phase is stable[7,8] with respect to the *normal* one for $T < T_c$.

Preprints (www.preprints.org) | NOT PEER-REVIEWED | Posted: 5 July 2022 doi:10.20944/preprints202207.0074.v1

Since the normal electrons make up a degenerate Fermi gas ($\Rightarrow T_c << E_F/k_B$ with k_B being Boltzmann's constant), the Sommerfeld expansion[15] can be used up to T^2 and yields

$$E_F(T_c,c_0) = E_F(0,c_0) - \frac{\rho'}{\rho}\frac{(\pi k_B T_c)^2}{6}$$
$$\frac{\partial E_F}{\partial c_n}(T_c,c_0) = \left(\rho + \rho''\frac{(\pi k_B T_c)^2}{6}\right)^{-1} \quad , \qquad (11)$$

with $\rho = \rho(E_F(0,c_0)), \rho' = \frac{d\rho}{dE_F}(E_F(0,c_0)), \rho'' = \frac{d^2\rho}{dE_F^2}(E_F(0,c_0))$. Likewise, the following results have been worked out[5,6]

$$\mu(K, c_s = 0) = \frac{\varepsilon_0(K)}{2}$$
$$\frac{\partial\mu}{\partial c_s}(K, c_s = 0) = -\frac{\int_{-\pi}^{\pi}\frac{dk}{2\pi(\varepsilon_0(K)-\varepsilon(K,k))^3}}{2\left(\int_{-\pi}^{\pi}\frac{dk}{2\pi(\varepsilon_0(K)-\varepsilon(K,k))^2}\right)^2} \quad . \qquad (12)$$

The T_c dependence on U_0/t will be discussed by assuming the following *one-electron* density of states

$$\rho(\epsilon) = \frac{2}{\pi t_0\sqrt{1-\left(\frac{\epsilon}{t_0}\right)^2}} \quad ,$$

with $\epsilon \in [-t_0, t_0]$ ($\Rightarrow \int_{-t_0}^{t_0}\rho(\epsilon)d\epsilon = 2$ electrons per atomic site). Remarkably, the condition $\rho'(E_F(T_c,c_0)) > 0$ in Eq.(9) requires $c_0 > 1$, whereas the *opposite* condition $c_0 < 1$ must be fulfilled in the three-dimensional case[8].

Combining Eqs.(9,10,11,12) yields[8] finally a system of two equations

$$E_F - \frac{\rho'}{\rho}\frac{(\pi k_B T_c)^2}{6} - \frac{\varepsilon_0(K)}{2} = 0$$
$$\left(\rho + \rho''\frac{(\pi k_B T_c)^2}{6}\right)^{-1} + \frac{\partial\mu}{\partial c_s}(K, c_s = 0) = 0 \quad , \qquad (13)$$

to be solved for the unknowns $K(E_F,T_c), U_0(E_F,T_c)$ with

$$E_F = E_F(T = 0, c_0) \quad , \quad c_0 = \int_0^{E_F}\rho(\epsilon)d\epsilon \quad ,$$

while T_c will be dealt with as a disposable parameter.

To begin with, starting values are needed for K, U_0 in order to launch Newton's procedure. To that end, let us choose $K = \pi, T_c = 0$, which implies[6], with help of Eqs.(7,10,11), $\varepsilon_0 = U_0 \Rightarrow E_F = \frac{U_0}{2}$, $\frac{\partial\mu}{\partial c_s}(K = \pi, c_s = 0) = -\frac{U_0}{2}$ and $\rho(E_F) = \frac{2}{U_0}$ and yields finally $\frac{U_0}{t_0} = \frac{2}{\sqrt{1+\left(\frac{2}{\pi}\right)^2}}$ and $c_0 = 1.64$ electrons per site. Then K can be assigned thanks to Eqs.(12,13). At last this K value is fed into Eq.(7) to determine U_0. The results are presented in table I.

Eqs.(13) are seen to have no solution $K \in [0,\pi]$ for $c_0 < 1.64$ and there is no $U_0 > 0$ for $c_0 > 1.74$, whereas $U_0 > 0$ has been known as a prerequisite for persistent currents[5], thermal equilibrium[6], occurrence of a second order transition[7,8] at the critical temperature T_c and the Josephson effect[9]. Likewise there is no solution for

TABLE I. Solutions $K(c_0,T_c)$, $U_0(c_0,T_c)$, $E_F(c_0,T_c)$ of Eqs.(13), calculated for H_0 at two T_c values, $T_1 = 10$K and $T_2 = 220$K, with $t_0 = .2t$ and $t = 1$eV; the unit for c_0 is the number of electrons per site.

c_0	$\frac{K(T_1)}{\pi}$	$\frac{U_0(T_1)}{t}$	$\frac{E_F(T_1)}{t}$	$\frac{K(T_2)}{\pi}$	$\frac{U_0(T_2)}{t}$	$\frac{E_F(T_2)}{t}$
1.64	.977	.33	.169	.914	.174	.16
1.66	.932	.27	.172	.908	.151	.162
1.68	.919	.242	.175	.904	.128	.164
1.7	.91	.219	.178	.9	.106	.165
1.72	.903	.198	.181	.897	.083	.1661
1.74	.897	.177	.184	.896	.062	.1662

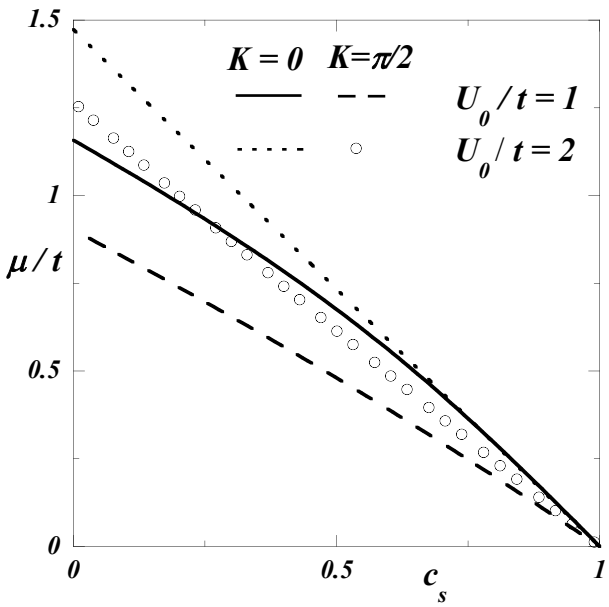

FIG. 4. Plots of $\mu(c_s)$, calculated for H_2 at $K = 0$ (solid and dotted line) and $K = \frac{\pi}{2}$ (dashed line and white circle) for $\frac{U_0}{t} = 1, 2$ and $U_1 = .2U_0$, $J = .1U_1$, respectively; c_s is the concentration of bound electrons, expressed as the number of electrons per site.

$T_c > 220$K. The main conclusion, drawn from table I, is that the inequality $U_0(T_2) < U_0(T_1)$ is indeed seen to hold for every c_0 value, in *qualitative agreement* with the observed, pressure induced[16–18] rise of T_c. A similar trend had been already noticed in the $d = 3$ case[8], for which $\frac{U_0(T_1=1K)}{U_0(T_2=300K)} - 1 > 0$ was yet found smaller than in the $d = 1$ case. This is likely to stem from the d-dependent behaviour of $\rho(\epsilon) \propto |\epsilon - \epsilon_{VH}|^{\frac{d}{2}-1}$ ($d = 1,2,3$) for ϵ close to a Van Hove singularity, located at ϵ_{VH}.

A similar analysis will now be applied to H_2. Each bound electron pair of energy $\eta(K)$, as plotted in Fig.3, turns[6] continuously into a *MBE* state Φ at finite concentration c_s. As recalled above for a single pair, the corresponding Schrödinger equation

$$(H_2 - N\mathcal{E})\,\Phi = 0$$

Preprints (www.preprints.org) | NOT PEER-REVIEWED | Posted: 5 July 2022 doi:10.20944/preprints202207.0074.v1

can be recast[21], but *only* for $N \to \infty$, into

$$(H_d + H_K^s - N\mathcal{E})\,\psi_K^s = 0 \quad .$$

There is $\psi_K^s \in S_K^s$ and the Hilbert space S_K^s is subtended[21] by a basis of many-pair states, such as $\prod_{i=1,..n} b^+_{s,K,k_i}|0\rangle$, with $n = \frac{Nc_s}{2}$ being the number of electron pairs.

Then, taking $\langle\psi_K^s|\psi_K^s\rangle = \langle\Phi|\Phi\rangle = 1$ yields $\mathcal{E}(c_s) = \langle\psi_K^s|\frac{H_d+H_K^s}{N}|\psi_K^s\rangle = \langle\Phi|\frac{H_2}{N}|\Phi\rangle$, which can be reckoned by implementing a variational procedure, developed elsewhere[6] for H_0. It is based on the following assumptions

$$\begin{array}{c} n_k = \langle\Phi|\, b^+_{s,K,k} b_{s,K,k}\,|\Phi\rangle \Rightarrow n = \sum_k n_k \\ f(k) = \sqrt{n_k\,(1-n_k)} \\ \langle\Phi|\, b^+_{s,K,k} b_{s,K,k'}\,|\Phi\rangle = f(k)f(k') \end{array} \quad .$$

Then $\mathcal{E}$ reads

$$\begin{array}{c} \mathcal{E} = \sum_k \varepsilon(K,k)\frac{n_k}{N} + U_0\Delta_0^2 + 2\left(U_1\left(\Delta_c^2+\Delta_s^2\right)\right. \\ \left. +J\left(\cos(K)\left(\Delta_c^2-\Delta_s^2\right)+2\sin(K)\Delta_c\Delta_s\right)\right) \\ \Delta_0 = \sum_k \frac{f(k)}{N} \\ \Delta_c = \sum_k \frac{\cos(k)f(k)}{N} \quad , \quad \Delta_s = \sum_k \frac{\sin(k)f(k)}{N} \end{array} .$$

Furthermore minimising $\mathcal{E}$ ($\Rightarrow d\mathcal{E} = 0$), under the constraint of c_s kept constant ($\Rightarrow dc_s = 0$), while taking[2] $n_k = \sin^2(\theta_k)$ with $\theta_k \in \left[0, \frac{\pi}{2}\right]$, yields

$$\begin{array}{l} \tan(2\theta_k)\left(\mu - \frac{\varepsilon(K,k)}{2}\right) = U_0\Delta_0 \\ \quad +2\left(\left(U_1\cos(k) + J\cos(K-k)\right)\Delta_c\right. \\ \quad \left. +\left(U_1\sin(k) + J\sin(K-k)\right)\Delta_s\right) \end{array} \quad . \qquad (14)$$

Due to $\mu = \frac{\partial\mathcal{E}}{\partial n_k}, \forall k$, the chemical potential μ, associated with the electrons making up the *MBE* state, plays also the role of a Lagrange multiplier[6]. Note that, in case of $U_1 = J = 0$, Eq.(14) gives indeed for θ_k the expression[6] worked out for H_0 . At last $\Delta_0, \Delta_c, \Delta_s$ can be recast as

$$\begin{array}{l} \Delta_0 = \int_{-\pi}^{\pi} \sin(2\theta_k)\frac{dk}{4\pi} \\ \Delta_c = \int_{-\pi}^{\pi} \sin(2\theta_k)\cos(k)\frac{dk}{4\pi} \\ \Delta_s = \int_{-\pi}^{\pi} \sin(2\theta_k)\sin(k)\frac{dk}{4\pi} \end{array} \quad . \qquad (15)$$

The system of Eqs.(15), comprising three transcendental equations in terms of three unknowns $\Delta_0(\mu), \Delta_c(\mu), \Delta_s(\mu)$ with $\theta_k(\mu)$ defined by Eq.(14), has been solved thanks to Newton's method. This has enabled us to calculate

$$c_s(\mu) = \int_{-\pi}^{\pi} \frac{\sin^2(\theta_k)}{\pi} dk \quad .$$

The resulting $\mu(c_s)$ data have been plotted in Fig.4. They share several common properties with similar data obtained[6] for H_0

- there is $\mu(c_s \to 0) \to \frac{\eta(K)}{2}$;
- $U_0 > 0$ implies $\frac{\partial\mu}{\partial c_s} < 0$, which has been recognised as the prerequisite, conditioning *all* aspects of superconductivity[5–9];
- $\frac{\partial\mu}{\partial c_s}$ depends weakly on c_s.

TABLE II. Solutions $K(c_0,T_c)$, $U_0(c_0,T_c)$, $E_F(c_0,T_c)$ of Eqs.(13), calculated for H_2 at two T_c values, $T_1 = 10$K and $T_2 = 160$K, with $t_0 = .2t$, $U_1 = .2U_0$, $J = .1U_1$ and $t = 1$eV; the unit for c_0 is the number of electrons per site.

c_0	$\frac{K(T_1)}{\pi}$	$\frac{U_0(T_1)}{t}$	$\frac{E_F(T_1)}{t}$	$\frac{K(T_2)}{\pi}$	$\frac{U_0(T_2)}{t}$	$\frac{E_F(T_2)}{t}$
1.64	.926	.226	.169	.914	.167	.164
1.66	.918	.205	.172	.909	.147	.167
1.68	.911	.188	.175	.904	.128	.169
1.7	.905	.171	.178	.899	.108	.171
1.72	.9	.156	.181	.895	.088	.173
1.74	.895	.139	.184	.892	.068	.175

Eqs.(13) can now be solved for H_2, with $\eta(K)$ showing up instead of $\varepsilon_0(K)$, and the resulting data are available in table II. Note that there is no solution for $T_c > 160$K. Meanwhile they are close to those of table I, which concurs with the weak dependence of $\eta(K)$ on U_1, J, illustrated by Fig.3. In particular, the inequality $U_0(T_2) < U_0(T_1)$ is seen to hold again, in qualitative agreement with the measurements, carried out under high pressure[16–18]. They hint also at a practical route to achieve higher T_c values at ambient pressure. Accordingly, there are, in most superconducting materials, several one-electron bands, crossing $E_F(c_0,T_c)$ and pertaining to different symmetry classes of the crystal point group[8]. Hence, were it possible to sort out that one, contributing at most to $\rho(E_F)$ and the corresponding atoms, associated with the hopping integral t, it would be tempting to substitute them for isovalent atoms, so as to cause the lattice parameter to shrink, in order to see whether this might give rise to increasing T_c.

V. CONCLUSION

It has been concluded that *triplet* bound electron pairs are unlikely to arise in *three-dimensional* metals, unlike *singlet* pairs, the properties of which are conditioned primarily by the on-site Coulomb integral $U_0 > 0$. The prominent role of the *repulsive* Hubbard Hamiltonian in the whole realm of superconductivity is thereby ascertained.

Nevertheless, the weaker Coulomb repulsion between electrons, located at neighbouring sites, has proven instrumental in shifting T_c upward with decreasing U_0/t, which agrees qualitatively with observed pressure induced effect. Likewise, indirect two-electron couplings, such as mediated by electron-phonon (known[1,2] to be influential on the isotope effect) or electron-spin

 doi:10.20944/preprints202207.0074.v1

interaction[22–24], may also alter T_c and the corresponding T_c behaviour could be assessed by working out the effective two-electron potential, as done elsewhere[7], and then solving the relevant Eqs.(13), as done above for H_0, H_2.

At last, since the Coulomb repulsion governs the electron motion in metals, one might wonder why not *every* metallic compound is superconducting. It is not so, because solutions of Eq.(10) can be found, but inside a *narrow* range of c_0, U_0 values, as illustrated by the data in tables I,II. Remarkably, T_c has a Hamiltonian dependent, upper bound.

Acknowledgements

The author is beholden to M. Abou Ghantous and the Referee for help and encouragement.

[1] Parks R.D.: Superconductivity, CRC Press (1969)
[2] Tinkham M.: Introduction to Superconductivity, Dover Books (2004)
[3] Cooper L.N.: Phys. Rev., 104, 1189 (1956)
[4] Bardeen J., Cooper L.N. and Schrieffer J.R.: Phys.Rev., 108, 1175 (1957)
[5] Szeftel J., Sandeau N. and M. Abou Ghantous M.: Eur.Phys.J.B, 92, 67 (2019)
[6] Szeftel J., Sandeau N. and M. Abou Ghantous M.: J.Supercond.Nov.Magn., 33, 1307 (2020)
[7] Szeftel J., Sandeau N., Abou Ghantous M. and El-Saba M.: J.Supercond.Nov.Magn., 34, 37 (2021)
[8] Szeftel J., Sandeau N., Abou Ghantous M. and El-Saba M.: EuroPhys.Lett., 134, 27002 (2021)
[9] Szeftel J., Sandeau N. and Abou Ghantous M.: J.Supercond.Nov.Magn., 35, 65 (2022)
[10] Ishida K. *et al.*: Nature, 396, 658 (1998)
[11] Duffy J.A. *et al.*: Phys.Rev.Lett. 85, 5412 (2000)
[12] Szeftel J., Sandeau N., Khater A.: Prog.Electromagn.Res.M, 69, 69 (2018)
[13] Szeftel J., Abou Ghantous M., Sandeau N.: Prog.Electromagn.Res.L., 81, 1 (2019)
[14] Szeftel J., Sandeau N., Abou Ghantous M., Khater A.: EuroPhys.Lett., 131, 17003 (2020)
[15] Ashcroft N.W. and Mermin N. D.: Solid State Physics, Saunders College (1976)
[16] Snider E. *et al.*: Nature, 586, 373 (2020)
[17] Grinenko V. *et al.*: Nat.Phys., 17, 1254 (2021)
[18] Eremets M.I. *et al.*: J.Supercond.Nov.Magn., 35, 965 (2022)
[19] Lorenz B., Chu C. W.: Frontiers in Superconducting Materials, A. V. Narlikar (Ed.), Springer Berlin Heidelberg (2005) (also available at *arXiv* : cond-mat/0410367)
[20] Eliashberg G. M.: Soviet Phys.JEPT, 12, 1000 (1961)
[21] Szeftel J.: J.Supercond.Nov.Magn., 35, 689 (2022)
[22] Armitage N.P., Fournier P. and Greene R.L.: Rev.Mod.Phys., 82, 2421 (2010)
[23] Zaanen J.: 100 years of superconductivity, eds. Rochalla H. and Kes P.H., Chapman and Hall (2011) (also available at *arXiv* : 1012.5461)
[24] Lederer P.: *arXiv* : 1510.08808